Dopamine-Related Disruption of Functional Topography of Striatal Connections in Unmedicated Patients With Schizophrenia

Guillermo Horga, MD, PhD; Clifford M. Cassidy, PhD; Xiaoyan Xu, PhD; Holly Moore, PhD; Mark Slifstein, PhD; Jared X. Van Snellenberg, PhD; Anissa Abi-Dargham, MD

IMPORTANCE Despite the well-established role of striatal dopamine in psychosis, current views generally agree that cortical dysfunction is likely necessary for the emergence of psychotic symptoms. The topographic organization of striatal-cortical connections is central to gating and integration of higher-order information, so a disruption of such topography via dysregulated dopamine could lead to cortical dysfunction in schizophrenia. However, this hypothesis remains to be tested using multivariate methods ascertaining the global pattern of striatal connectivity and without the confounding effects of antidopaminergic medication.

OBJECTIVES To examine whether the pattern of brain connectivity across striatal subregions is abnormal in unmedicated patients with schizophrenia and whether this abnormality relates to psychotic symptoms and extrastriatal dopaminergic transmission.

DESIGN, SETTING, AND PARTICIPANTS In this multimodal, case-control study, we obtained resting-state functional magnetic resonance imaging data from 18 unmedicated patients with schizophrenia and 24 matched healthy controls from the New York State Psychiatric Institute. A subset of these (12 and 17, respectively) underwent positron emission tomography with the dopamine D_2 receptor radiotracer carbon 11–labeled FLB457 before and after amphetamine administration. Data were acquired between June 16, 2011, and February 25, 2014. Data analysis was performed from September 1, 2014, to January 11, 2016.

MAIN OUTCOMES AND MEASURES Group differences in the striatal connectivity pattern (assessed via multivariable logistic regression) across striatal subregions, the association between the multivariate striatal connectivity pattern and extrastriatal baseline D_2 receptor binding potential and its change after amphetamine administration, and the association between the multivariate connectivity pattern and the severity of positive symptoms evaluated with the Positive and Negative Syndrome Scale.

RESULTS Of the patients with schizophrenia (mean [SEM] age, 35.6 [11.8] years), 9 (50%) were male and 9 (50%) were female. Of the controls (mean [SEM] age, 33.7 [8.8] years), 10 (42%) were male and 14 (58%) were female. Patients had an abnormal pattern of striatal connectivity, which included abnormal caudate connections with a distributed set of associative cortex regions ($\chi^2_{29} = 53.55$, $P = .004$). In patients, more deviation from the multivariate pattern of striatal connectivity found in controls correlated specifically with more severe positive symptoms ($\rho = -0.77$, $P = .002$). Striatal connectivity also correlated with baseline binding potential across cortical and extrastriatal subcortical regions ($t_{25} = 3.01$, $P = .01$, Bonferroni corrected) but not with its change after amphetamine administration.

CONCLUSIONS AND RELEVANCE Using a multimodal, circuit-level interrogation of striatal-cortical connections, it was demonstrated that the functional topography of these connections is globally disrupted in unmedicated patients with schizophrenia. These findings suggest that striatal-cortical dysconnectivity may underlie the effects of dopamine dysregulation on the pathophysiologic mechanism of psychotic symptoms.

Author Affiliations: Department of Psychiatry, Columbia University College of Physicians and Surgeons, New York, New York (Horga, Cassidy, Xu, Moore, Slifstein, Van Snellenberg, Abi-Dargham); Division of Translational Imaging, New York State Psychiatric Institute, New York (Horga, Cassidy, Xu, Slifstein, Van Snellenberg, Abi-Dargham); Division of Integrative Neuroscience, New York State Psychiatric Institute, New York (Moore).

Corresponding Author: Guillermo Horga, MD, PhD, New York State Psychiatric Institute, Columbia University Medical Center, 1051 Riverside Dr, Unit 31, New York, NY 10032 (horgag@nyspi.columbia.edu).

The striatum, in particular the associative striatum, is a central pathologic site in schizophrenia.[1] Excessive dopamine in the associative striatum is an established finding in unmedicated patients with schizophrenia in whom the capacity for amphetamine-induced dopamine release correlates with worsening of psychotic symptoms.[2,3] Such striatal excess of dopamine is thought to mediate its effects on cognition via basal ganglia-thalamocortical (BGTC) circuits, which normally modulate cortical function by gating incoming information to the cortex.[4] A topographic organization within the BGTC circuits is thus crucial for anatomically selective gating of information to relevant cortical targets,[5,6] and its disruption could produce various symptoms characteristic of schizophrenia.

In normal conditions, cortical inputs to the striatum are topographically organized in semiparallel loops.[5,7] In addition, hot spot territories of converging inputs exist in the associative striatum that may be necessary to integrate disparate sources of reward and cognitive information.[8,9] In schizophrenia, although the pairwise connectivity of specific striatal subregions with other brain regions has been assessed to some extent with univariate functional magnetic resonance imaging (fMRI) analyses, it is largely unknown whether such functional topography of striatal connections as a whole (ie, the global pattern of connections across striatal subregions rather than connection strengths between specific pairs of striatal subregions and extrastriatal regions) is disrupted.

A key modulator of synaptic connectivity and plasticity in the striatum is dopamine.[10] Indeed, a fundamental role of dopamine in learning depends on its ability to modulate synaptic plasticity[11-14] and thus the functional efficacy of neuronal connections at striatal synapses and elsewhere. Therefore, excessive dopamine transmission in the associative striatum could disrupt the organization of striatal-cortical connections, ultimately leading to aberrant information processing and psychosis. Disrupted connectivity could be further compounded by a deficit in extrastriatal dopamine, as recently found in schizophrenia.[15] At the same time, the established effects of dopamine on striatal connectivity in healthy participants[16,17] suggest that antipsychotic drugs may critically mask underlying abnormalities in striatal connectivity in medicated patients. Because this confounder may affect most fMRI connectivity studies conducted in medicated patients with schizophrenia, it is therefore imperative to examine this question in unmedicated patients.

We investigated the pattern of resting-state functional connectivity across subregions of the striatum in unmedicated patients with schizophrenia and healthy controls using a multivariate approach. Our main aims were to test whether the functional topography of striatal connections is altered in schizophrenia and whether such abnormalities correlate with severity of psychotic symptoms and with amphetamine-induced dopamine release and dopamine D_2 receptor (D_2R) density.

Methods

Participants

Unmedicated patients with schizophrenia (n = 19) and healthy controls (n = 24) were recruited at the New York State Psychi-

Key Points

Question Is the overall pattern of striatal connections with the rest of the brain abnormal in schizophrenia and does it relate to symptoms and extrastriatal dopamine parameters?

Findings In this multimodal functional magnetic resonance imaging and positron emission tomography study, 18 unmedicated patients with schizophrenia had an abnormal pattern of striatal connectivity compared with 24 healthy controls, an abnormality that correlated with severity of positive symptoms and with lower extrastriatal dopamine D_2 receptor density.

Meaning Abnormal striatal-cortical circuitry in schizophrenia may play an important role in the pathophysiologic mechanisms of psychosis and relates to lower extrastriatal dopamine D_2 receptor function.

atric Institute and through advertisements. All participants provided written informed consent as approved by the institutional review boards of the New York State Psychiatric Institute and Yale University, and data were deidentified. Inclusion criteria for healthy controls were absence of any *DSM-IV* Axis I diagnosis and of psychotic illness in first-degree relatives. Inclusion criteria for patients were lifetime *DSM-IV* diagnosis of schizophrenia or schizoaffective or schizophreniform disorder (based on the Diagnostic Interview for Genetic Studies[18] and consensus diagnosis), no antipsychotics for 3 weeks before study enrollment, and no violent behavior. Common exclusion criteria were significant medical illnesses, misuse of substances other than nicotine, positive urine drug screen result, pregnancy, and nursing. Positron emission tomography (PET) and task-based fMRI data on 28 of the 42 study participants were previously published.[15]

Symptom severity was assessed with the Positive and Negative Syndrome Scale (PANSS), the Scale for the Assessment of Positive Symptoms (SAPS),[19] and the Scale for Assessment of Negative Symptoms (SANS).[20] The Hollingshead scale,[21] the Edinburgh Handedness Inventory,[22] and the MATRICS (Measurement and Treatment Research to Improve Cognition in Schizophrenia) Consensus Cognitive Battery[23] were also administered.

Resting-State fMRI Data Acquisition

Participants completed 2 runs of 165 volumes each on a 1.5-T scanner (Koninklijke Philips NV). They were instructed to relax and keep their eyes open. Participants were spoken to before and after each sequence to ensure wakefulness. Whole-brain functional echoplanar images were obtained using an 8-channel coil (3-mm isotropic voxels; eMethods in the Supplement).

fMRI Preprocessing

Preprocessing followed standard procedures in SPM8 (Wellcome Trust Centre for Neuroimaging) and scrubbing procedures for resting-state fMRI[24] (eMethods in the Supplement). Scrubbing cutoffs were established based on a larger data set for 2 indexes of motion-related data quality reflecting the rate

of change in brain-wide signal (DVARS) and total instantaneous framewise displacement (FD), respectively. One patient was excluded because of excessive motion. Temporal band-pass filtering, spatial smoothing, and voxelwise z scoring of time series were applied.

Region-of-Interest Definition

Striatal and extrastriatal regions of interest (ROIs) were manually drawn on individual T1-weighted scans as defined previously.[25,26] The striatum was divided into 5 subregions: (1) ventral striatum, (2) anterior (precommissural) caudate, (3) posterior (postcommissural) caudate, (4) anterior putamen, and (5) posterior putamen. Unsmoothed fMRI data from each subregion were averaged across the containing voxels (collapsing across hemispheres; eMethods in the Supplement) and z scored to construct seed time series. Extracting the first eigenvariate instead of the mean yielded almost identical results, indicating high functional homogeneity within subregions. Ipsilateral and contralateral connectivity was highly consistent within subregions (eMethods in the Supplement).

fMRI Data Analysis

Participant-level analyses consisted of a generalized linear model in SPM8, including the following regressors: spatially averaged time series for each of the 5 striatal subregions (seeds) (regressors 1-5),[27] time series for white matter and cerebrospinal fluid regions of no interest (eMethods in the Supplement) (regressors 6-7), 6 head motion (realignment) parameters and their first derivatives[24] (all band-pass filtered) (regressors 8-19), and run and global intercepts (regressors 20-21). One dummy variable was additionally included to censor each artifactual set of adjacent volumes exceeding the DVARS or FD cutoffs. The resulting regression coefficient (β) maps for each striatal subregion, representing connection strengths for each brain voxel with 1 striatal subregion while controlling for the other 4 (and the nuisance variables), were used subsequently.

Multivariate fMRI Analyses

Our primary goal was to test whether the overall pattern of striatal connectivity predicted group membership using logistic regression. We used a multivariate approach rather than univariate analyses because the latter can only test connectivity between individual seeds and target regions but not the overall (multivariate) pattern of connectivity across seeds. Our purpose in using logistic regression, however, was not as a diagnostic classifier but rather as a test of multivariate differences in connectivity. Exploratory analyses (eMethods in the Supplement) used a multivariate recursive feature elimination support vector machine classifier for the former purpose.

First, whole-brain connectivity β maps for each striatal subregion were parcellated into Brodmann areas (BAs) and subcortical nuclei using the Talairach Daemon Atlas in the Wake Forest University PickAtlas toolbox[28,29] (henceforth referred to as target regions), after excluding striatal voxels. Second, a data-reduction step retained only target regions that exhibited significant connectivity with any of the striatal subregions ($P \leq .005$, uncorrected, in ≥20% of the voxels) in either group; 29 regions met these criteria (for individual striatal sub-

regions 1-5, the number of target regions to meet criteria were 0, 24, 2, 5, and 4, respectively). Although these selection criteria were unbiased toward any subregion, they yielded more target regions for the anterior caudate given its stronger widespread connectivity.

Next, logistic regression was used to predict group membership based on connection strengths for striatal-target pairs (ie, individual mean connectivity β values for each target region by striatal subregion). Because including all pairs as predictor variables would result in an underdetermined model, we used model building with step-forward selection to progressively include sets of predictor variables, with each of 5 possible sets consisting of all connectivity β values for target regions significantly associated with a given striatal subregion. Models that consisted of predictors from 1 set at a time were analyzed, and the set that resulted in the lowest P value was retained. Additional sets of variables were retained in the model if they significantly improved the model fit ($P < .05$, likelihood ratio test). The likelihood ratio test for the final model was our a priori test of group differences in connectivity patterns (other P values were used only for data-reduction and model-building steps). Once the final model was determined, the participantwise predicted log odds of belonging to the healthy group based on the multivariate connectivity pattern was used as a summary index of degree of abnormality in the striatal connectivity pattern for further correlational analyses with clinical and PET data (note that these analyses were unbiased because the ordering of the log odds across individuals was orthogonal to all clinical and PET data except for group membership, which was controlled for appropriately; eMethods in the Supplement).

These correlational analyses used parametric tests except when the data were not normally distributed (based on a Lilliefors test), in which case nonparametric tests were used. Spearman rank (partial) correlations were used to assess the association between connectivity and severity of positive symptoms within patients based on the PANSS positive total (PANSS-PT) scores, while controlling for negative symptoms as measured by the PANSS negative total (PANSS-NT) scores. Robust multiple linear regression (iteratively reweighted least squares with bisquare-weighting function) was used to assess the association between connectivity and PET data across all participants while controlling for group and nuisance variables. Spearman rank correlations were used for exploratory analyses of the MATRICS composite score. Effects surviving a $P = .05$ are reported. Bonferroni correction for multiple comparisons was used when necessary. Finally, the number of artifactual volumes regressed out for each participant was also used as an fMRI data quality score.

PET Preprocessing and Data Analysis

A detailed description of PET procedures and results was previously published.[15] Participants underwent 2 PET scans with the D_2 radiotracer carbon 11-labeled FLB457 on an HR+ scanner (Siemens) at Yale University: a baseline scan and another scan 3 hours after oral administration of amphetamine (0.5 mg/kg). Arterial plasma was collected to form metabolite-corrected input functions. Kinetic modeling used a 2-tissue compartment model that incorporated a set of shared param-

Table. Sociodemographic, Clinical, and Other Relevant Characteristics of Healthy Controls and Patients With Schizophrenia[a]

Characteristic	Controls (n = 24)	Patients (n = 18)	P Value[b]
Age, mean (SEM), y	33.7 (8.8)	35.6 (11.8)	.54
Sex			
Male	10 (42)	9 (50)	.59
Female	14 (58)	9 (50)	
Race/ethnicity			
White	6 (25)	1 (6)	
African American	8 (33)	9 (50)	
Hispanic	5 (21)	4 (22)	.28
Asian	3 (15)	1 (6)	
Mixed	2 (8)	2 (11)	
Parental SES	39.0 (13.9)	45.6 (11.7)	.13
Handedness			
Right	23	16	.39
Left	1	2	
Nicotine smoking			
No	21	13	.21
Yes	3	5	
PANSS, mean (SEM) [range]			
Positive total score [range, 7-49]	7.0 (0.0) [7-8]	13.6 (6.4) [9-23]	<.001
Negative total score [range, 7-49]	8.8 (1.4) [7-16]	15.1 (5.8) [7-25]	<.001
General total score [range, 16-112]	17.0 (1.4) [16-25]	29.1 (7.8) [18-53]	<.001
MATRICS Consensus Cognitive Battery composite T scores	46.3 (2.5)	33.3 (3.7)	.02
Medication status (drug naive or drug free)	...	6/12	...
Onset psychotic symptoms, y	...	16.4 (5.2)	...
Duration of psychotic illness, y	...	18.7 (12.2)	...
Censored data (No. of scrubbed volumes)	64.3 (13.5)	99.5 (21.7)	.16
FD after censoring[c]	0.29 (0.0)	0.30 (0.0)	.76
Interval between fMRI and PET, d	20.5 (24.8)	7.2 (2.6)	.67

Abbreviations: ellipses, data not applicable; FD, framewise displacement; fMRI, functional magnetic resonance imaging; MATRICS, Measurement and Treatment Research to Improve Cognition in Schizophrenia; PANSS, Positive and Negative Syndrome Scale; PET, positron emission tomography; SES, socioeconomic status.

[a] Data are presented as number (percentage) of participants unless otherwise indicated. All 18 patients met *DSM-IV* criteria for schizophrenia (vs other disorders in the schizophrenia spectrum). See eTable 1 in the Supplement for the subset of participants with fMRI and PET data. See eTable 2 in the Supplement for PET scanning parameters and additional data.

[b] P values correspond to 2-sample *t* tests for continuous variables and χ^2 tests for categorical variables.

[c] Mean FD is given for scrubbed fMRI frames.

eter estimates across predefined ROIs.[25,26] Binding potential (BP$_{ND}$) and its relative change from baseline after amphetamine (ΔBP$_{ND}$) were estimated in each ROI excluding the striatum; striatal BP$_{ND}$ cannot be quantified with [^{11}C]FLB457 because of its slow washout in this high D$_2$R density region. Both BP$_{ND}$ and ΔBP$_{ND}$ values were highly correlated across regions (mean *r* of approximately 0.8). Thus, as a data reduction step, we performed principal component analyses with varimax rotation, separately for BP$_{ND}$ and ΔBP$_{ND}$, across regions. Horn's parallel analyses[30] yielded a 1-factor solution for baseline BP$_{ND}$ (corresponding to D$_2$R density across all regions) and a 1-factor solution for ΔBP$_{ND}$ (corresponding to dopamine release across all regions). For correlational analyses, individual factor scores were calculated as the weighted sum of factor loadings by the PET measures (BP$_{ND}$ or ΔBP$_{ND}$) across ROIs.

Results

### Sociodemographic and Clinical Characteristics

Groups were matched for sociodemographic characteristics, nicotine smoking, and head motion after scrubbing (**Table**). Clinical characteristics are also given in the Table.

Functional Topography of Striatal Connections (Multivariate fMRI Analysis)

The pattern of connection strengths across striatal-target pairs differed numerically between the groups, particularly for the anterior caudate (**Figure 1**). Statistically, the logistic regression model that best explained group membership (χ^2_{29} = 53.55, P = .004, likelihood ratio [omnibus] test) was one that included all connection pairs related to the anterior caudate (with 24 pairs) and posterior caudate (with 5 pairs) (Figure 1). Thus, the pattern of functional connections between the caudate and specific regions of the cortex and thalamus was abnormal in patients. Cortical regions that individually contributed to this effect included prefrontal (BAs 8, 10, and 44), sensory association (BAs 20, 22, 19, and 7), posterior cingulate (BA 23), and entorhinal (BA 28) cortices. The log odds of belonging to the healthy group did not relate to medication status or age (P = .20 and P = .23, respectively).

Alternative definitions of the relevant target regions yielded similar results (eMethods in the Supplement). Additional analyses suggested that, although connectivity patterns for each striatal subregion could separately predict group membership, the pattern associated with the posterior cau-

Figure 1. Differences in Multivariate Patterns of Striatal Connections Between Unmedicated Patients With Schizophrenia and Healthy Controls
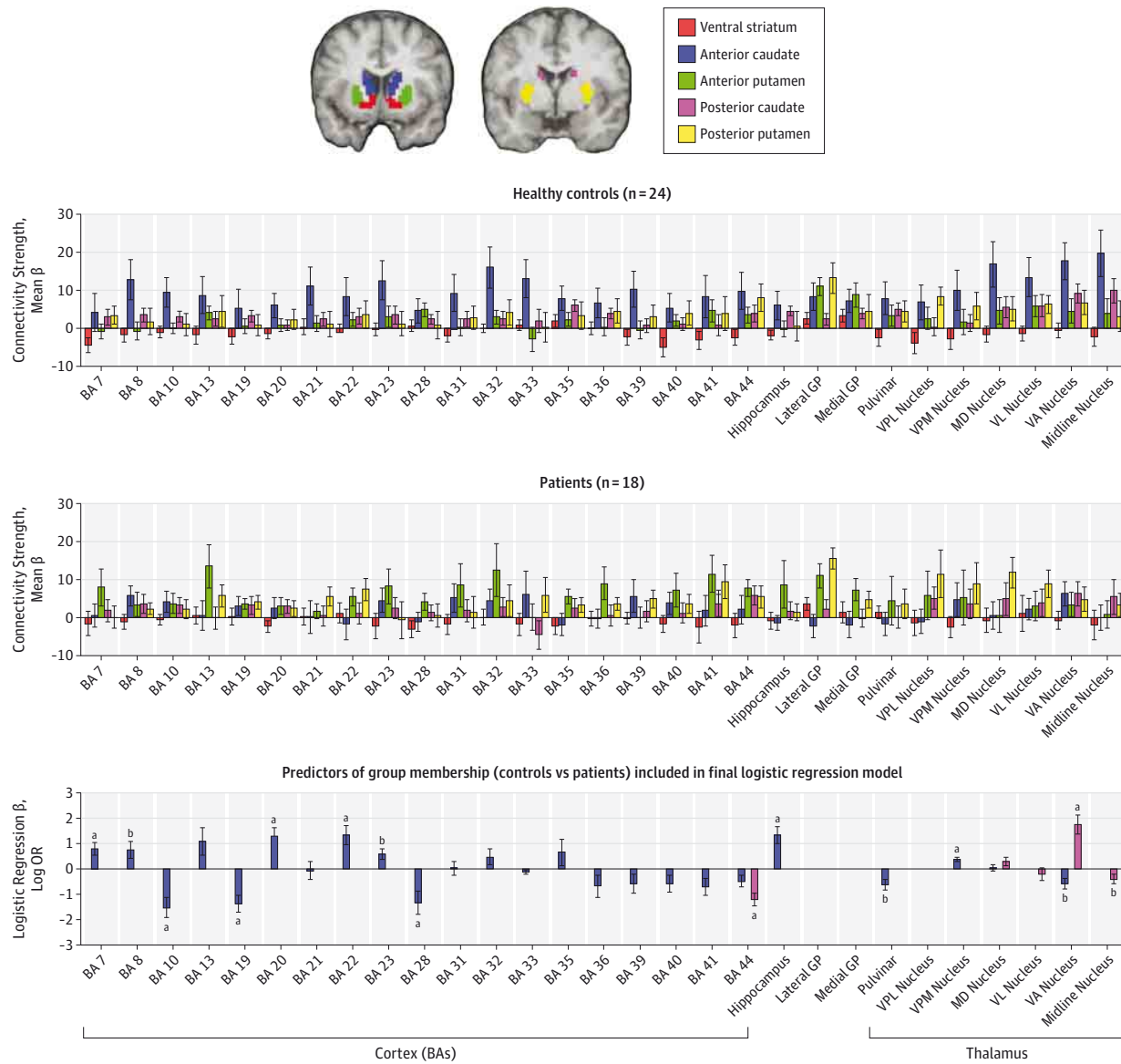
Top, Coronal views of striatal subregion seeds; voxels identified as part of each subregion in at least half of the study participants are overlaid on a group-averaged T1-weighted image. Middle, Patterns of striatal connectivity are shown in controls (top) and patients (bottom) as bar plots of connectivity strength (group mean [SEM] β) by striatal subregion (using the same color scheme as in the top panel) and target region on the x-axis (from left to right, cortical Brodmann areas [BAs] followed by hippocampus, globus pallidus, and thalamic nuclei). Bottom, β weights (log odds ratio [OR]) corresponding to each of the predictor variables or regressors included in the final logistic regression model predicting group membership (1 indicates controls and 0 indicates patients); this final (most parsimonious) model included only striatal-target

pairs related to the anterior caudate and posterior caudate (eMethods in the Supplement). P values indicate logistic regression β estimates significantly different than zero (post hoc tests of individual β estimates adjusted their degrees of freedom based on the total number of predictor variables, thus controlling for multiple comparisons). GP indicates globus pallidus; MD, mediodorsal; VA, ventral anterior; VL, ventrolateral; VPL, ventral posterior lateral nucleus; VPM, ventral posterior medial.

[a] $P < .01$.

[b] $P < .05$.

date was the most discriminative (eMethods in the Supplement). Finally, a recursive feature elimination support vector machine classifier discriminated patients and controls above chance based on the global pattern of striatal connectivity (including pairs for all subregions except for the ventral striatum; eFigure in the Supplement).

Clinical Correlations

Patients with a more abnormal (less controllike) striatal connectivity pattern (ie, lower log odds of belonging to the healthy control group) had more severe positive symptoms (PANSS-PT: $\rho = -0.76$, $P = .001$; SAPS: $\rho = -0.66$, $P = .008$) (Figure 2). This correlation was not observed with negative symptoms

Figure 2. Correlations of Striatal Connectivity Pattern With Symptom Severity and D_2 Receptor Density Measured With Carbon 11–Labeled FLB457 Positron Emission Tomography (PET)
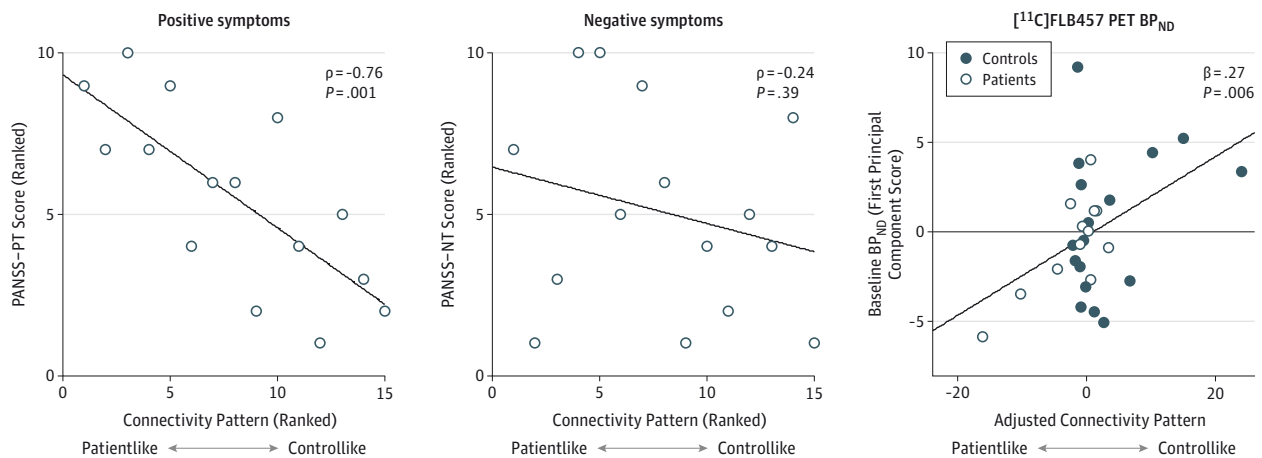
Scatterplots show associations between connectivity pattern (log odds of belonging to the healthy group based on the multivariate pattern of striatal connectivity) and severity of positive symptoms based on the Positive and Negative Syndrome Scale positive total (PANSS-PT) scores, severity of negative symptoms based on the Positive and Negative Syndrome Scale negative total (PANSS-NT) scores, and baseline binding potential (BP_{ND}) (corresponding to the first principal component score), adjusted by group and functional magnetic resonance imaging data quality score across all participants (note that group adjustment shifts the group means such that the connectivity pattern appears to overlap between the groups along the x-axis). For positive and negative symptoms, values are ranked across subjects given that the appropriate corresponding tests are nonparametric. [^{11}C] indicates radiotracer carbon 11–labeled.

(PANSS-NT: $\rho = -0.24$, $P = .39$; SANS: $\rho = 0.01$, $P = .96$) (Figure 2). Furthermore, the correlation with PANSS-PT held after controlling for PANSS-NT and fMRI data quality scores ($\rho = -0.77$, $P = .002$). Alternative analyses cross-validated this finding (eMethods in the Supplement). The PANSS-PT and PANSS-NT scores were not correlated among patients ($\rho = 0.31$, $P = .26$).

Correlations With [^{11}C]FLB457 PET Measures

We found that more controllike striatal connectivity patterns correlated with higher baseline BP_{ND} principal component scores, even after adjusting for fMRI data quality scores and group ($\beta = .27$, $t_{25} = 3.01$, $P = .006$, $P = .01$, Bonferroni corrected) (Figure 2) but no interaction of connectivity pattern by group or significant associations with ΔBP_{ND}. Excluding a potentially influential outlier did not alter this result ($P = .002$). This effect was also apparent within patients only ($P = .005$) and was corroborated by alternative analyses and across individual regions (eMethods in the Supplement). Age was unrelated to the PET measures ($P = .12$ and $P = .48$ for baseline and ΔBP_{ND}, respectively). Baseline BP_{ND} principal component scores were similar in both groups ($t_{27} = 0.76$, $P = .45$).

Exploratory Correlations With Neurocognitive Measures

Exploratory analyses revealed a correlation between abnormal striatal connectivity patterns and worse MATRICS composite scores in patients ($\rho = 0.68$, $P = .03$) but not in controls.

Exploratory Analyses of Univariate Voxelwise Functional Connectivity and Global Brain Connectivity

A test of the group by striatal subregion interaction and the group effects for individual subregions did not yield significant results (eMethods in the Supplement). In healthy controls, but not in patients, the anterior caudate had a significantly stronger connectivity than any of the other subregions to prefrontal, parietal, and temporal association cortices, as well as to the thalamus ($P = .001$, $P = .003$, $P = .003$, and $P = .001$, respectively, false discovery rate corrected) (Figure 3). However, the group difference was not significant. Finally, the anterior caudate had higher global brain connectivity (eMethods in the Supplement) or weighted degree centrality, a graph theoretic index of hubness, than the other striatal subregions ($P < .001$, $= .02$, $P < .001$, and $P = .001$ for ventral striatum, anterior putamen, posterior caudate, and posterior putamen, respectively) (Figure 4). The global brain connectivity of the anterior caudate was numerically but not significantly reduced in patients (eMethods in the Supplement).

Discussion

Our results indicate that the normal functional topography of striatal connections, particularly but not solely of caudate connections, is disrupted in schizophrenia. Because our sample was exclusively composed of unmedicated patients, this disruption is unlikely attributable to antipsychotic medication and may instead be relevant to the pathophysiologic mechanisms of schizophrenia. Further supporting this interpretation, abnormal striatal connectivity correlated with clinical severity, specifically with severity of positive symptoms but not negative symptoms. Finally, abnormal connectivity also correlated with lower density of D_2Rs across cortical and extrastriatal subcortical brain regions within the same individuals.

Our results converge in suggesting that the healthy caudate, in particular the anterior caudate, is a connectivity

Figure 3. Voxelwise Connectivity of Striatal Subregions in Patients and Healthy Controls
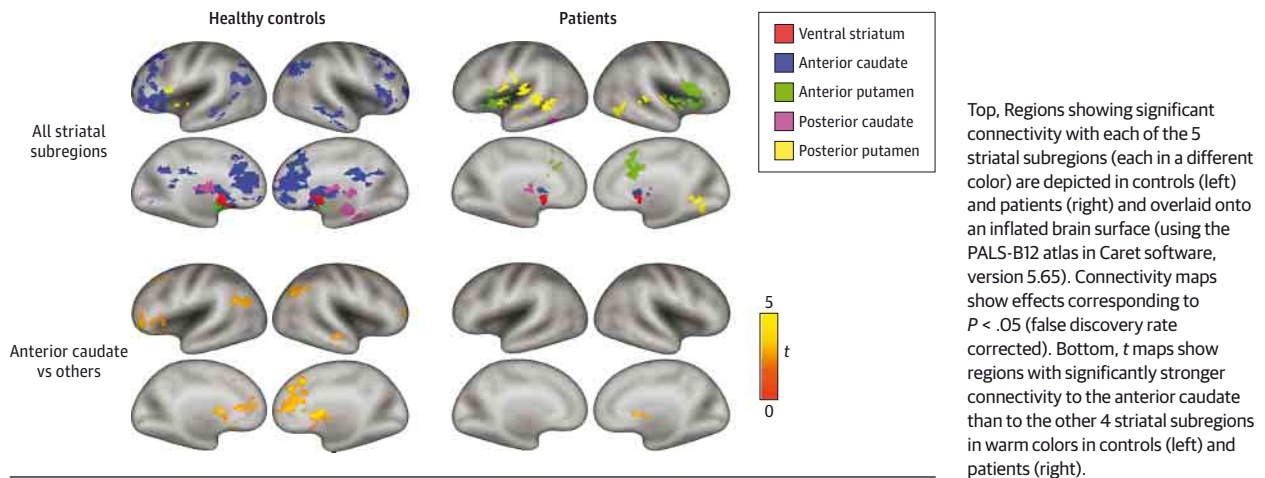

Top, Regions showing significant connectivity with each of the 5 striatal subregions (each in a different color) are depicted in controls (left) and patients (right) and overlaid onto an inflated brain surface (using the PALS-B12 atlas in Caret software, version 5.65). Connectivity maps show effects corresponding to $P < .05$ (false discovery rate corrected). Bottom, t maps show regions with significantly stronger connectivity to the anterior caudate than to the other 4 striatal subregions in warm colors in controls (left) and patients (right).

Figure 4. Global Brain Connectivity of Striatal Subregions in Patients and Healthy Controls
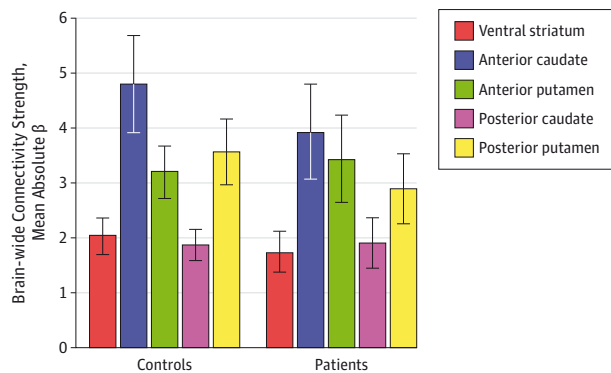
Mean (SEM) absolute β values across all extrastriatal brain voxels are plotted by striatal subregion and group.

hub. In health, connectivity of the anterior caudate with an extended set of higher-order associative regions was stronger than that of other striatal subregions. In contrast, this primacy of the anterior caudate was not as apparent in patients. The pattern observed in health is consistent with previous work indicating that the anterior caudate receives overlapping projections from various regions in frontoparietal cortices.[31] This previous work suggests that in addition to the semisegregated loops supporting specialization,[5] convergence zones within the anterior caudate may serve as information-processing hubs relevant for integration.[32]

Given this, our results of abnormal striatal connectivity patterns in schizophrenia and its association with positive symptoms may suggest that a disruption that affects, among other regions, a striatal hub for information multiplexing is involved in psychosis, in line with dysconnectivity hypotheses.[33] Our findings may be consistent with findings of disrupted hemispheric specialization[34] and decreased global connectivity of the caudate,[35] as well as those indicating deficient striatocortical connectivity in schizophrenia[36-39] and altered caudate-

cortical connectivity in individuals at high risk for psychosis.[37,40] Although dysfunction[41] and dysconnectivity[42] of the (ventral) striatum may relate to negative symptoms, we failed to find such an association, although more work in this direction is warranted. Together with findings highlighting the role of striatal dopamine dysregulation in schizophrenia,[1] our results suggest that disruptions of striatal circuitry may plausibly mediate the deleterious effects of dopamine dysregulation on cortical processes involved in perception and cognition.[43-45]

Our PET results indeed suggest that abnormal striatal connectivity in schizophrenia may depend on dopamine. We failed to detect an association between dysconnectivity and amphetamine-induced dopamine release, possibly because of the limited range of extrastriatal release in patients, who had a marked deficit in release with preserved D_2R levels.[15] However, we observed more abnormal connectivity associated with lower baseline density of D_2R across extrastriatal regions. Prefrontal dopamine exerts a bidirectional modulation of network activity by tuning recurrent network excitation, where D_2 stimulation reduces inhibitory postsynaptic currents.[46,47] Therefore, decreased D_2Rs could potentially explain aberrant network activity propagating through BGTC circuits and leading to disruptions in activity-dependent plasticity consistent with the observed pattern of dysconnectivity in patients. Furthermore, the generalized deficit in extrastriatal dopamine release in patients[15] is likely to compound lower D_2R expression, further dampening dopamine D_2 function in those patients with more manifest dysconnectivity. Finally, the observed associations among D_2R, deficient striatal connectivity, and psychosis are consistent with a study[48] that reported that improvement of psychosis after D_2R-blocking medication correlated with strengthened caudate-prefrontal connectivity.

Our study has several limitations. The limited sample size may have increased the risk of false-negative results and effect size inflation. Our choice of radiotracer precluded measures of striatal dopamine and of D_1R, which would lead to a better understanding of the association between dopamine and dysconnectivity. Nonetheless, this is, to our

knowledge, the first multimodal study in schizophrenia that combines molecular imaging and a systems-level fMRI connectivity approach. Exploratory univariate analyses failed to find a group difference in contrast to our primary multivariate analysis. However, this finding could suggest that multivariate measures provide a more powerful way to interrogate circuit pathologic mechanisms. Finally, a general limitation of resting-state studies is the lack of control over transient mental states experienced during data collection. Although we did not debrief participants after scanning, psychotic symptoms experienced in the scanner tend to correlate highly with prescanning severity scores.[44] Thus, our findings related to psychosis severity may partly reflect psychopathologic states experienced in the scanner.

Conclusions

Unmedicated patients with schizophrenia have abnormalities in the functional topography of striatal connections. These abnormalities correlate specifically with more severe psychotic symptoms and lower density of extrastriatal D_2R, suggesting the relevance of this neural phenotype to the pathophysiologic mechanisms of psychosis and potentially informing new therapeutic targets at the intersection between molecules and neural systems. Our results further suggest that the striatum contains connectivity hubs relevant for cognitive integration whose disruption may impair higher-order cortical processes involved in psychosis.

REFERENCES

1. Howes OD, Kambeitz J, Kim E, et al. The nature of dopamine dysfunction in schizophrenia and what this means for treatment. *Arch Gen Psychiatry*. 2012;69(8):776-786.

2. Laruelle M, Abi-Dargham A, Gil R, Kegeles L, Innis R. Increased dopamine transmission in schizophrenia: relationship to illness phases. *Biol Psychiatry*. 1999;46(1):56-72.

3. Thompson JL, Urban N, Slifstein M, et al. Striatal dopamine release in schizophrenia comorbid with substance dependence. *Mol Psychiatry*. 2013;18(8):909-915.

4. Carlsson A. The current status of the dopamine hypothesis of schizophrenia. *Neuropsychopharmacology*. 1988;1(3):179-186.

5. Alexander GE, DeLong MR, Strick PL. Parallel organization of functionally segregated circuits linking basal ganglia and cortex. *Annu Rev Neurosci*. 1986;9:357-381.

6. Lawrence AD, Sahakian BJ, Robbins TW. Cognitive functions and corticostriatal circuits: insights from Huntington's disease. *Trends Cogn Sci*. 1998;2(10):379-388.

7. Haber SN. The primate basal ganglia: parallel and integrative networks. *J Chem Neuroanat*. 2003;26(4):317-330.

8. Averbeck BB, Lehman J, Jacobson M, Haber SN. Estimates of projection overlap and zones of convergence within frontal-striatal circuits. *J Neurosci*. 2014;34(29):9497-9505.

9. Haber SN, Kim KS, Mailly P, Calzavara R. Reward-related cortical inputs define a large striatal region in primates that interface with associative cortical connections, providing a substrate for incentive-based learning. *J Neurosci*. 2006;26(32):8368-8376.

10. Surmeier DJ, Plotkin J, Shen W. Dopamine and synaptic plasticity in dorsal striatal circuits controlling action selection. *Curr Opin Neurobiol*. 2009;19(6):621-628.

11. Centonze D, Picconi B, Gubellini P, Bernardi G, Calabresi P. Dopaminergic control of synaptic plasticity in the dorsal striatum. *Eur J Neurosci*. 2001;13(6):1071-1077.

12. Charpier S, Deniau JM. In vivo activity-dependent plasticity at cortico-striatal connections: evidence for physiological long-term potentiation. *Proc Natl Acad Sci U S A*. 1997;94(13):7036-7040.

13. Frank MJ. Dynamic dopamine modulation in the basal ganglia: a neurocomputational account of cognitive deficits in medicated and nonmedicated Parkinsonism. *J Cogn Neurosci*. 2005;17(1):51-72.

14. Pawlak V, Kerr JN. Dopamine receptor activation is required for corticostriatal spike-timing-dependent plasticity. *J Neurosci*. 2008;28(10):2435-2446.

15. Slifstein M, van de Giessen E, Van Snellenberg J, et al. Deficits in prefrontal cortical and extrastriatal dopamine release in schizophrenia: a positron emission tomographic functional magnetic resonance imaging study. *JAMA Psychiatry*. 2015;72(4):316-324.

16. Cole DM, Oei NY, Soeter RP, et al. Dopamine-dependent architecture of cortico-subcortical network connectivity. *Cereb Cortex*. 2013;23(7):1509-1516.

17. Kelly C, de Zubicaray G, Di Martino A, et al. L-dopa modulates functional connectivity in striatal cognitive and motor networks: a double-blind placebo-controlled study. *J Neurosci*. 2009;29(22):7364-7378.

18. Nurnberger JI Jr, Blehar MC, Kaufmann CA, et al; NIMH Genetics Initiative. Diagnostic interview for genetic studies. Rationale, unique features, and training. *Arch Gen Psychiatry*. 1994;51(11):849-859.

19. Andreasen NC. *Scale for the Assessment of Positive Symptoms (SAPS)*. Iowa City: University of Iowa; 1984.

20. Andreasen NC. *Scale for the Assessment of Negative Symptoms (SANS)*. Iowa City: University of Iowa; 1983.

21. Hollingshead AB. *Four Factor Index of Social Status*. New Haven, CT: Working paper published by the author; 1975.

22. Oldfield RC. The assessment and analysis of handedness: the Edinburgh inventory. *Neuropsychologia*. 1971;9(1):97-113.

23. Nuechterlein KH, Green MF, Kern RS, et al. The MATRICS Consensus Cognitive Battery, part 1: test selection, reliability, and validity. *Am J Psychiatry*. 2008;165(2):203-213.

24. Power JD, Barnes KA, Snyder AZ, Schlaggar BL, Petersen SE. Spurious but systematic correlations in functional connectivity MRI networks arise from subject motion. *Neuroimage*. 2012;59(3):2142-2154.

25. Abi-Dargham A, Xu X, Thompson JL, et al. Increased prefrontal cortical D1 receptors in drug naive patients with schizophrenia: a PET study with [11C]NNC112. *J Psychopharmacol*. 2012;26(6):794-805.

26. Abi-Dargham A, Martinez D, Mawlawi O, et al. Measurement of striatal and extrastriatal dopamine D1 receptor binding potential with [11C]NNC 112 in humans: validation and reproducibility. *J Cereb Blood Flow Metab*. 2000;20(2):225-243.

27. Di Martino A, Scheres A, Margulies DS, et al. Functional connectivity of human striatum: a resting state FMRI study. *Cereb Cortex*. 2008;18 (12):2735-2747.

28. Lancaster JL, Woldorff MG, Parsons LM, et al. Automated Talairach atlas labels for functional brain mapping. *Hum Brain Mapp*. 2000;10(3):120-131.

29. Maldjian JA, Laurienti PJ, Kraft RA, Burdette JH. An automated method for neuroanatomic and cytoarchitectonic atlas-based interrogation of fMRI data sets. *Neuroimage*. 2003;19(3):1233-1239.

30. Horn JL. A rationale and test for the number of factors in factor analysis. *Psychometrika*. 1965;30: 179-185.

31. Jarbo K, Verstynen TD. Converging structural and functional connectivity of orbitofrontal, dorsolateral prefrontal, and posterior parietal cortex in the human striatum. *J Neurosci*. 2015;35 (9):3865-3878.

32. Haber SN, Behrens TE. The neural network underlying incentive-based learning: implications for interpreting circuit disruptions in psychiatric disorders. *Neuron*. 2014;83(5):1019-1039.

33. Stephan KE, Friston KJ, Frith CD. Dysconnection in schizophrenia: from abnormal synaptic plasticity to failures of self-monitoring. *Schizophr Bull*. 2009;35(3):509-527.

34. Mueller S, Wang D, Pan R, Holt DJ, Liu H. Abnormalities in hemispheric specialization of caudate nucleus connectivity in schizophrenia. *JAMA Psychiatry*. 2015;72(6):552-560.

35. Argyelan M, Ikuta T, DeRosse P, et al. Resting-state fMRI connectivity impairment in schizophrenia and bipolar disorder. *Schizophr Bull*. 2014;40(1):100-110.

36. Quidé Y, Morris RW, Shepherd AM, Rowland JE, Green MJ. Task-related fronto-striatal functional connectivity during working memory performance in schizophrenia. *Schizophr Res*. 2013;150(2-3):468-475.

37. Fornito A, Harrison BJ, Goodby E, et al. Functional dysconnectivity of corticostriatal circuitry as a risk phenotype for psychosis. *JAMA Psychiatry*. 2013;70(11):1143-1151.

38. Koch K, Rus OG, Reeß TJ, et al. Functional connectivity and grey matter volume of the striatum in schizophrenia. *Br J Psychiatry*. 2014;205 (3):204-213.

39. Zhou Y, Liang M, Jiang T, et al. Functional dysconnectivity of the dorsolateral prefrontal cortex in first-episode schizophrenia using resting-state fMRI. *Neurosci Lett*. 2007;417(3):297-302.

40. Dandash O, Fornito A, Lee J, et al. Altered striatal functional connectivity in subjects with an at-risk mental state for psychosis. *Schizophr Bull*. 2014;40(4):904-913.

41. Radua J, Schmidt A, Borgwardt S, et al. Ventral striatal activation during reward processing in psychosis: a neurofunctional meta-analysis. *JAMA Psychiatry*. 2015;72(12):1243-1251.

42. Reckless GE, Andreassen OA, Server A, Østefjells T, Jensen J. Negative symptoms in schizophrenia are associated with aberrant striato-cortical connectivity in a rewarded perceptual decision-making task. *Neuroimage Clin*. 2015;8:290-297.

43. Horga G, Parellada E, Lomeña F, et al. Differential brain glucose metabolic patterns in antipsychotic-naïve first-episode schizophrenia with and without auditory verbal hallucinations. *J Psychiatry Neurosci*. 2011;36(5):312-321.

44. Horga G, Schatz KC, Abi-Dargham A, Peterson BS. Deficits in predictive coding underlie hallucinations in schizophrenia. *J Neurosci*. 2014;34 (24):8072-8082.

45. Jardri R, Pouchet A, Pins D, Thomas P. Cortical activations during auditory verbal hallucinations in schizophrenia: a coordinate-based meta-analysis. *Am J Psychiatry*. 2011;168(1):73-81.

46. Durstewitz D, Seamans JK, Sejnowski TJ. Dopamine-mediated stabilization of delay-period activity in a network model of prefrontal cortex. *J Neurophysiol*. 2000;83(3):1733-1750.

47. Trantham-Davidson H, Neely LC, Lavin A, Seamans JK. Mechanisms underlying differential D1 versus D2 dopamine receptor regulation of inhibition in prefrontal cortex. *J Neurosci*. 2004;24 (47):10652-10659.

48. Sarpal DK, Robinson DG, Lencz T, et al. Antipsychotic treatment and functional connectivity of the striatum in first-episode schizophrenia. *JAMA Psychiatry*. 2015;72(1):5-13.